Optimised co-registration of multi-contrast spinal cord data and application to multi-parameter mapping

Rebecca S Samson[1], Laura Brightman[2], Olga Ciccarelli[3], Carolina Kachramanoglou[3], Antoine Lutti[4], David J L Thomas[5], Nikolaus Weiskopf[4], and Claudia A M Wheeler-Kingshott[1]

[1]NMR Research Unit, Department of Neuroinflammation, UCL Institute of Neurology, London, England, United Kingdom, [2]University of Cambridge, Cambridge, United Kingdom, [3]NMR Research Unit, Department of Brain Repair and Rehabilitation, UCL Institute of Neurology, London, England, United Kingdom, [4]Wellcome Trust Centre for Neuroimaging, UCL Institute of Neurology, London, England, United Kingdom, [5]Department of Brain Repair and Rehabilitation, UCL Institute of Neurology, London, England, United Kingdom

INTRODUCTION: The spinal cord (SC) is a common site of involvement in neurological disorders such as multiple sclerosis (MS). High field post mortem MRI studies have demonstrated focal and diffuse abnormalities in cord white (WM) and grey matter (GM) (1). Myelin content and axonal density in MS cord WM have also been shown to correlate with T_1, T_2, proton density (PD) and Magnetisation Transfer Ratio (MTR) at high field (2,3). However, performing tissue-specific quantitative cord MRI measurements *in vivo* is challenging due to its small cross-sectional size and the potential for cord motion during the scan. There is currently no established method for co-registration of axial multi-parametric SC MRI data, although some studies have co-registered data of the same contrast either axially (4) or sagittally (5). However, this is an important issue for quantitative measurement methods, and protocols incorporating different MRI contrasts.

We tested a number of options for registration of spinal cord data previously acquired as part of a multi-parameter mapping study (6) using the linear registration tool of the FSL (www.fmrib.ox.ac.uk/fsl) software package (FLIRT). The optimum registration method was used to co-register the multi-parametric data in 13 healthy volunteers and column-specific region-of-interest (ROI) parameter values at cord level C2 are presented here.

METHODS: ***MRI acquisition:*** 13 subjects (12M, 1F, aged 36.4±12.3) were scanned on a 3T Magnetom TIM Trio scanner (Siemens Healthcare, Erlangen, Germany) with a head, neck and spine receiver coil. 80 3mm thick partitions were acquired, with axial field-of-view (FOV)=200mmx200mm, 256x256 acquisition matrix, sinc interpolated in image space to 512x512, and phase encoding anterior/posterior (A/P), with GRAPPA acceleration factor 2 in the phase encoding direction. A slab selective 3D multi-echo FLASH sequence (7, 8) was performed 3 times, with PD (PDw; TR=24.05ms, flip angle (α)=6º) , MT (MTw; acquired with an additional 4ms off-resonance Gaussian RF pulse (nominal α=220º, offset frequency 2kHz) before each excitation pulse) or T_1 (T_1w; TR=22ms, α=20º) weighting. The spatial distribution of the B_1 transmit field was measured using a modified 3D actual flip angle imaging (AFI) method (9) with alternative RF/gradient spoiling scheme (10), with two excitation pulses of α =60° followed by delays of 50 and 150ms and a gradient echo readout at TE=3.05ms. 40 6mm partitions were acquired, with FOV=200mmx200mm, and acquisition matrix 64x64, i.e. pixel size 3.13x3.13, sinc interpolated to 0.39x0.39, to enable correction of the T_1 maps.

SC registration optimisation*:* For a single subject, cord levels C1-C5 were extracted using FSL and averaged PDw and T1w images were registered to MTw data, using FSL's linear registration tool FLIRT, testing a number of different options: degrees of freedom (DOF) = 3, 6 or 12; cost function = correlation ratio, mutual information or normalised mutual information, and interpolation = tri-linear, sinc or nearest neighbour, varying one parameter at a time.

Following registration of the PDw and T1w to the target MTw image, the 3 (co-registered) images were 'averaged' (the T1w image contrast was inverted to match the PDw/MTw images, i.e. CSF brighter than the spinal cord). This 'average' image was then used as a new registration target and all the 3 original images were registered to it, in order to ensure no bias was introduced in the final images due to the registration process.

Overlaid co-registered images and subtraction maps (Figure 1: MTw-PDw (a,b), MTw-T1w (c,d) & PDw-T1w (e,f)) were visually assessed, and the optimised registration method selected as the best was used to register the multi-parameter mapping data for all 13 subjects. B_1 data were also co-registered to the (registered) T_1w data using 6DOF and mutual information as a cost function, to enable correction of T_1 maps. Parameter maps were then calculated, providing A, MT, R_2^*, T_1 and MTR, according to a previously reported model (6, 7, 8) (figure 2). 4 ROIs were placed manually using Jim 6.0 (www.xinapse.com) in the dorsal, left (L) and right (R) lateral columns and GM (figure 2 (MTw)) over 5 slices at the C2 level of the cervical cord similarly to (11) and applied to the parameter maps.

Table 1: Mean parameter values for 13 subjects

A (±SD) (a. u.)	MT (±SD) (pu)	MTR (±SD) (pu)	R_2^* (±SD) (s^{-1})	T_1 (±SD) (ms)
4668 (±699)	1.43 (±0.15)	44.5 (±1.9)	22.3 (±3.04)	1735 (±205)
4792 (±947)	1.43 (±0.15)	43.7 (±2.5)	20.5 (±2.35)	1707 (±219)
4408 (±583)	1.47 (±0.15)	44.6 (±2.2)	21.2 (±2.61)	1593 (±221)
5160 (±910)	1.18 (±0.11)	40.6 (±2.6)	18.9 (±1.96)	1815 (±170)

Figure 1: Example subtraction (MTw-PDw) (a,b), MTw-T1w (c,d) & PDw-T1w (e,f) maps without (left) and with (right) registration. Significant motion between the T1w &MTw/PDw scans can be observed (see arrows), but is somewhat resolved following registration.

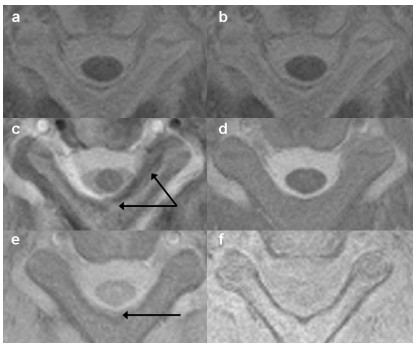

RESULTS: The most appropriate registration option for this data was to use the combination of normalised mutual information as the cost function, 6 DOF and sinc interpolation. We also compared registration of full FOV images with 'cut' rectangular ROI images just encompassing the whole cord, but little difference in registration was observed, therefore full FOV images were used for subsequent registrations. Example subtraction maps (MTw-PDw, MTw-T1w, PDw-T1w) without (a,c,e) and with (b,d,f) registration are given in figure 1; note the significant original displacement between the T1w scan and MTw/PDw images (see arrows), adjusted by the registration.

Example MTw images (with example ROI placement indicated) and parameter maps from a single subject at cervical cord level C2 are shown in figure 2. Mean parameter values are given in table 1. WM parameter values are comparable to those previously obtained for the whole spinal cord (6) and MTR values are similar to those previously obtained using a 3T Siemens system (4). All parameter values were shown to be significantly different in GM compared to WM regions via paired t-tests ($p<0.05$).

Since ROIs placed in WM and GM columns in the SC are very small, displacements of just 1-2 voxels would render quantitative ROI measurements in the cord impossible, and cord motion of this order could easily be expected given the duration of the scans acquired here.

CONCLUSIONS: We investigated various linear registration methods within the FSL software package for co-registration of multi-modal cervical cord data and the optimum method was selected via visual assessment of subtraction maps. The optimal method was used to register multi-modal data prior to estimation of multi-parametric maps in 13 healthy subjects, and parameter values in different WM columns and GM were measured over 5 slices at the C2 cervical level. Significant differences in the parameter values between WM and GM regions were found, demonstrating that it is feasible to make tissue-specific multi-parametric measurements in the cord using the method described to register the multi-modal data. Future work will include investigating the registration method in pathology, as well as investigating SC registration for other MRI contrasts.

Figure 2: Example MTw image with approximate ROI placement indicated (red=lateral, blue=dorsal column, yellow=GM), and parameter maps: A, MT, MTR, R_2^*&T_1

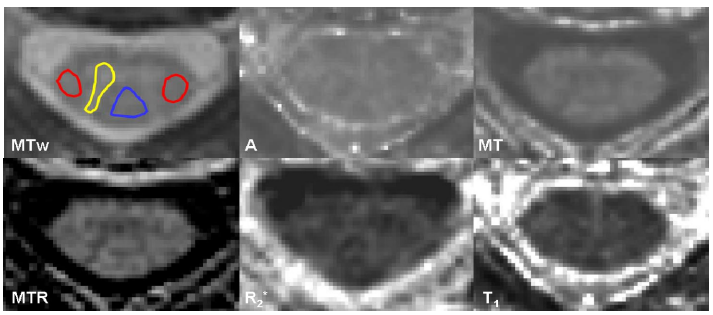

REFERENCES: [1] Gilmore CP *et al* Mult Scler 15: 180-188 (2009), [2] Mottershead JP *et al* J Neurol 250: 1293-1301 (2003), [3] Bot JCJ *et al* Radiology 233: 531-540 (2004), [4] Cohen-Adad J *et al* NeuroImage 55:1024-33 (2011) [5] Stroman PW *et al* MRI 26: 809-14 (2008), [6] Samson RS *et al* Proc ISMRM 19: 2754 (2011), [7] Weiskopf N & Helms G Proc ISMRM 16: 2241 (2008), [8] Helms G *et al* MRM 59:667-72 (2008), [9] Yarnykh V MRM 57 (1): 192-200 (2007), [10] Lutti A *et al* MRM 64: 229-38 (2010), [11] Smith SA *et al* MRM 61: 22-27 (2009)

Acknowledgements: The authors would like to thank the MS Society of Great Britain and Northern Ireland, the Wellcome Trust and the CBRC for support.